

SUB-PIXEL IMAGE CLASSIFICATION OF HYPER-SPECTRAL DATA FOR VEGETATION AND SOIL MAPPING IN SEMI-ARID ENVIRONMENT

Muhammad Kamal

m.kamal@geo.ugm.ac.id

*Department of Geographic Information Sciences and Regional Development,
Faculty of Geography, Gadjah Mada University*

ABSTRACT

The HyMap hyper-spectral data was used to classify photosynthetic vegetation (PV), non-photosynthetic vegetation (NPV), and exposed soils in a semi-arid savannah environment of McKinlay, northern Queensland, and Australia. This study aimed to understand how effective the sub-pixel classification approach applied on hyper-spectral data to distinguish the vegetation and soil features in semi-arid environment. In contrast to the per-pixel approach, this approach treats the pixel value as reflectance sum of its composite features, and shows its component abundance. The most commonly used sub-pixel classification technique was used in this research, namely Linear Spectral Unmixing (LSU). End members were used as the input class, and the result was compared with the standard maximum likelihood classification (MLC) using post-classification comparison method. The result of this study shows that LSU produced a patchy distribution of classes throughout the image. The brown soil tends to be over-estimated with respect to other classes. PV features were relatively well-mapped compare to other classes. NPV features have problem with domination of exposed soil reflectance. This is equivalent to the previous studies result that background soil dominates the spectral reflectance in this environment. According to the qualitative accuracy assessment, LSU has higher accuracy in representing PV and NPV compare to the traditional MLC classification.

Keywords: sub-pixel, hyper-spectral, linear spectral unmixing, semi-arid

INTRODUCTION

Arid and semi-arid environments cover approximately 35% of the earth's land surface, and have important function for grazing, wildlife habitat, irrigated agriculture, mining, solar energy generation, wood fuels, recreation, military bases, etc. Remote sensing technology has been employed to study in these areas for decades. However, mapping land cover in these areas using remote sensing imageries is problematic, due to their unique environment [McGwire *et al.*, 2000;

Okin et al., 2001]. The particular challenges in mapping in these areas are including the relatively low proportion of vegetation cover, the predominance of perennial species which often have low photosynthetic activity, patchiness of the environment, and the mixture of vegetation and soil reflectance [*Lewis*, 2000; *Asner & Heidebrecht*, 2002].

Arid and semi-arid regions have cloud-free weather and generally have bright spectral properties along with high air and surface temperatures, high evapotranspiration rates and sparse vegetation [*Tueller*, 1987]. The problem of quantitative retrieval of vegetation and soil features in this area arises from several factors, those are;

1. Individual plant canopies are typically small [*Lewis*, 2000; *Asner & Heidebrecht*, 2002],
2. A large soil background which can dominate the reflectance/absorption contribution of plant and the potential of nonlinear mixing due to multiple scattering of light rays [*Okin et al.*, 2001],
3. Localized environment patchiness [*Lewis*, 2000],
4. Heterogeneity of vegetation species which leads to mixed pixels [*Tueller*, 1987],
5. Temporal change in vegetation state and soil signature [*Karnieli et al.*, 2002; *Bastin & Ludwig*, 2006], and
6. Problem at separating photosynthetic and non-photosynthetic vegetations from soil background [*Roberts et al.*, 1993; *Asner & Heidebrecht*, 2002].

Hyper-spectral remote sensing has potential capabilities in quantitative measurement of key feature properties of surface [*Hill et al.*, 2006]. Imaging spectroscopy is routinely used in applying land cover mapping and for detecting the impacts of land use on ecosystem. The increased spectral resolution of the data provides access to spectral absorption features that can be used in various classification methods [*Ustin et al.*, 2004]. It is a promising tool for the analysis of vegetation and soils in arid and semi-arid regions. Many studies have been carried out to investigate the ability of hyper-spectral data for vegetation and soil mapping in this environment [*Roberts et al.*, 1993; *Drake et al.*, 1999; *Lewis, et al.*, 2001; *Okin et al.*, 2001; *Asner & Heidebrecht*, 2002; *Karnieli et al.*, 2002].

Traditional classification methods, which assign each pixel to a certain cover class, are not always so suitable that they often result in a poor representation of reality. The nature of pixels value made up of some different cover materials is not well represented. A more suitable way of extracting information from such scenes is to estimate how each ground pixel's area is divided up among different cover types. This approach was usually known as mixture modeling.

An area assigned by a single pixel of remote sensing image usually contains a lot of different materials. These materials are mixed and the pixel reflectance observed by sensor was a combination of reflectance of individual materials. To get more information from a single pixel, the proportion of these materials can be approximated using a spectral unmixing model. Using this model the mixed pixel can be reconstructed from known spectra in the image or the mixed pixel can be divided into components.

This study assesses the capability of sub-pixel classification approach applied on HyMap Airborne hyper-spectral Image to map vegetation (photosynthetic and non-photosynthetic) and soil features in semi-arid environment. The classification technique used is Linear Spectral Unmixing (LSU). The background question in this study is whether the sub-pixel classification can explain better features group due to their heterogeneity than the traditional per-pixel classification.

THE METHODS

Study Area

The site of this study is part of McKinlay area, centered at 529610 E and 7648045 N (Fig.1, coordinate in GDA 1994 MGA Zone 54). It is a little town located at 104 kilometers southeast of Cloncurry, North West, Queensland. This region is predominantly (approximately 70%) grassland that is persistently dry or suffers from winter drought. Other climate types in this region include desert and subtropical. Average annual rainfall in this region varies from 200 mm in the inland areas, to more than 400 in the areas toward the coast. Average annual temperatures in this region range from a minimum of 9°C and a maximum of 24°C east of Charleville, to a minimum of 18°C and a maximum of 33°C in the north [Commonwealth of Australia, 2007].

The study area is located at Mitchell Grass Downs bioregion, which is characterized by undulating downs on shale and limestone with Mitchell grass (*Astrebla spp*) grasslands and *Acacia* low woodlands [Accad et al., 2006]. According to CRSSIS field data (2006), the dominant weeds in this area were mesquite (*Nahualt mizquitl*), parkinsonia (*Parkinsonia aculeate*), prickly acacia (*Acacia nilotica*), and mimosa bush (*Acacia farnesiana*). The soils are predominantly deep heavy gray and brown cracking clays often with self-mulching and sometimes stony surfaces. The plains are interspersed with drainage lines, supporting open grasslands, herb lands or eucalypt woodlands and isolated remnant plateaus supporting a variety of hummock grasslands and shrub land vegetation [Commonwealth of Australia, 2007].

Image Dataset

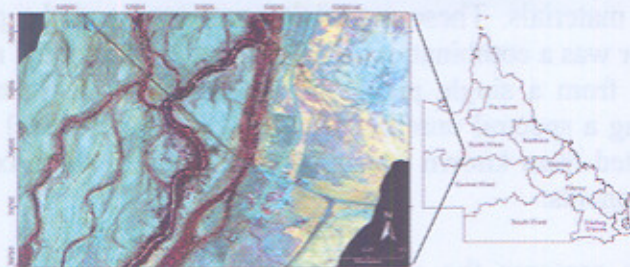


Figure 1. Study area, McKinlay, North West, Queensland, Australia

HyMap or Hyper-spectral Mapper is an advanced hyper-spectral sensor developed by Integrated Supertronics, Sydney Australia, representing the current state-of-the-art in airborne hyper-spectral remote sensing. The sensor covers the 0.45 – 2.5 μm region in 126, approximately 15- nm-wide spectral bands with 3-10m spatial resolution and signal-to-noise ratios of 500-1000 or better. The system is a whiskbroom scanner utilizing diffraction gratings and four 32-element detector arrays to provide 126 spectral channels covering the 0.45 – 2.5 μm range over a 512-pixel swath [Kruse *et al.*, 2000]. Table 1 summarizes the configuration and operational characteristics of the current HyMap sensor.

Table 1. HyMap configuration and operational characteristics [Cocks *et al.*, 1998]

Typical Sensor parameters	
Spectral regions	VIS, NIR, SWIR, MWIR, TIR
Number of channels	100 – 200
Spectral bandwidths	10 – 20 nm
Spatial resolution	2 – 10 m
Swath width	60 -70 degrees
Signal to noise ratio	>500:1
Typical operation Parameters	
Platform	Light, twin engine aircraft
Operation altitude	2000 – 5000 m AGL
Ground speeds	110 – 180 kts
Spatial Configuration	
IFOV	2.5 mr along track 2.0 mr across track
FOV	60 degrees (512 pixels)
Swath	2.3 km at 5m IFOV (along track) 4.6 km at 10m IFOV (along track)

This dataset has 126 bands and 4.9 m resolution, and was collected in August 2006. All scenes were processed atmospherically, geometrically and radio

metrically to at surface reflectance by the Centre of Remote Sensing and Spatial Information Science (CRSSIS), The University of Queensland. Geometrically, All scenes were projected into UTM coordinate system using MGA zone 54 southern hemisphere and GDA 1994 as the datum. Radio metrically, the at surface reflectance values were rescaled into the range of 0 to 10000, which means 100 percent of reflectance equals to 10000 DN on image. Acquisition date was chosen to reflect the optimum vegetation-soil exposure at the end of winter or early spring.

End member Selection

End member was developed for hyper-spectral-based classification method, which assigns the major materials found on image and have relatively pure reflectance [Lillesand *et al.*, 2004]. End member refers to a unique ground material and its spectra known as end member spectra. This class sampling was in the form of spectral signature of feature's properties, which was obtainable from laboratory or field spectra or extracted from the image for the known ground materials [Asner & Heidebrecht, 2002; Yang *et al.*, 2006].

This study intended to map major typical features found in semi-arid areas, those were photosynthetic vegetation (PV), non-photosynthetic vegetation (NPV; e.g. dry grass, leaf litter, and woody material), exposed soils (brown and gray soils), and road (asphalt). In selecting end members, some ancillary data were needed to assist the selection, which were the spectral reflectance of the feature to be mapped, vegetation and soils information, and fieldwork report. These data were required to get the suitable and accurate sample classes. A standard false color, true color bands compositions and NDVI image were found very useful in identifying the feature classes.

Classification Methods

Linear spectral unmixing method was developed to determine sub-pixel information. The input of this process was end members collected in the previous stage. This method assumed that a value at a given pixel was the result of a linear combination of one or more components. In the process of 'unmixing', this method estimated the fit of selected end members to the observed value of a pixel in order to estimate its proportion of composition. As a result, each pixel carried information about the predicted abundance of each of the end members [Okin *et al.*, 2001; Rosso *et al.*, 2005].

This mapping approach was based on assumption that the spectra of materials in an instrumental instantaneous field (IFOV) is combined linearly, with proportions given by their relative abundances. A combined spectrum thus can be decomposed into a linear mixture of its spectral end members [Okin *et al.*, 2001]. The weighting coefficients of each spectral end member, which must sum to one, were then interpreted as the relative area occupied by each material in a pixel (Fig. 2).

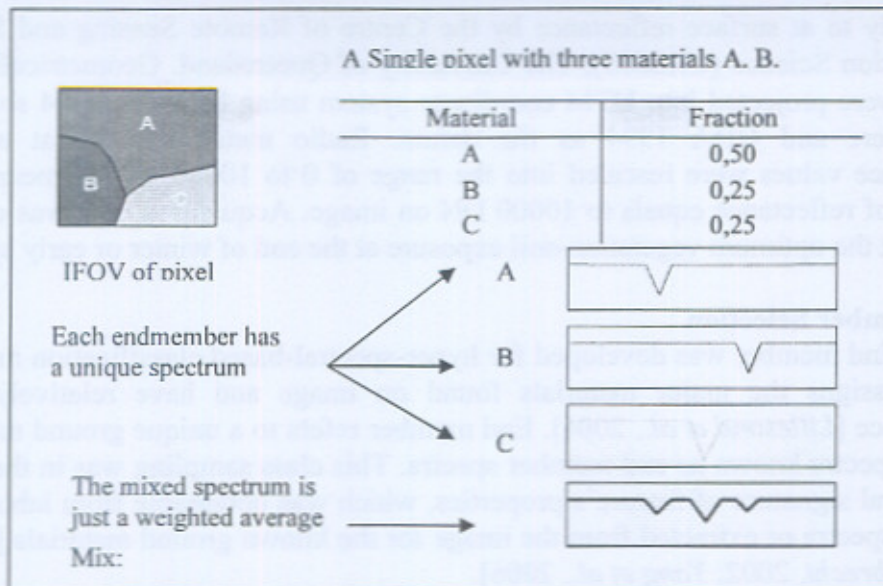


Figure 2. Principle of spectral mixing and unmixing [Van Der Meer & De Jong, 2001], with modificati

This method contrasts clearly with traditional classification approaches that assign only one possible value or category per pixel (i.e. maximum likelihood). Conceptually, it is deterministic method rather than statistical method, since it is based on a physical model of the mixture of discrete spectral response patterns [Lillesand *et al.*, 2004]. The results of this mapping method were classified maps of the approximate proportions of the ground area of each pixel that were occupied by each of the end member classes.

RESULTS AND DISCUSSION

PV, NPV, and Exposed Soil Discrimination

PV feature typically found as green vegetation could be identified as strong red color in FCC image, and associated with the streams. Spectrally, this feature can be identified by its high difference between red spectral absorption and NIR reflectance, due to the photosynthesis activity (Fig.3). NPV, on the other hand, usually lack significant quantities of chlorophyll and thus lack the high NIR to red contrast [Roberts *et al.*, 1993]. This category included materials such as dry leaf (dry grass and litter), bark, wood, and stems.

Supporting information derived from the image, such as NDVI, can also support the selection of these classes. Bright areas in NDVI image represent the dense vegetation canopy that can be assumed healthy green vegetation. The darker the area indicated the fewer the vegetation features exist. Exposed soil has a very distinct spectral reflectance compared to vegetation. It has higher reflectance at

most of the wavelength but less peak and valley. According to [Lillesand *et al.*, 2004], this is because the factors that influence soil reflectance act over less specific spectral bands.

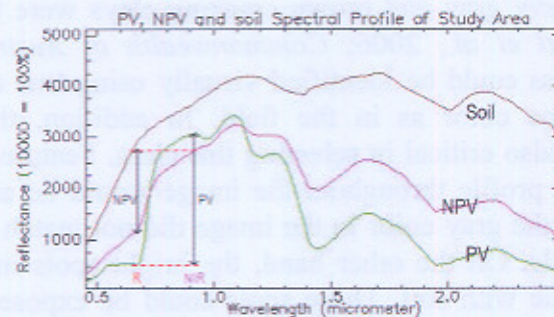


Figure 3. Spectral profiles of PV, NPV, and soil extracted from HyMap Image of the study area.

End member Selection

End members were selected as objects' reference spectra for LSU classification. There were some sources of end member; laboratory measurement, field spectra collection, or the one extracted from the image for the known ground materials [Asner & Heidebrecht, 2002; Yang *et al.*, 2006]. This study developed end members from the image data. Image-based end members were ideal because they were drawn from the population of data points to be analyzed, which increased the likelihood that image pixels will be decomposed using end members which actually exist in the area [Asner & Heidebrecht, 2002].

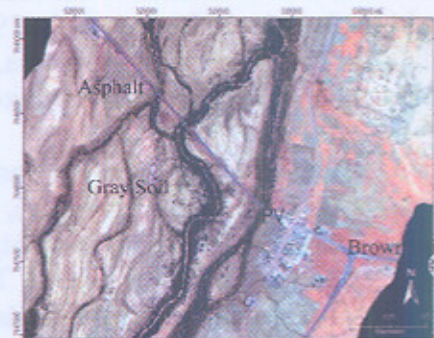
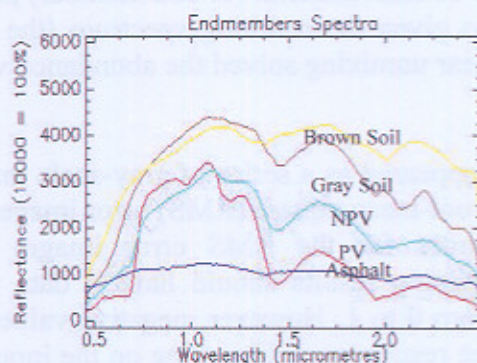


Figure 4. End member's spectra collection and their source locations (Indicated by + marks)

As discussed earlier, PV feature typically found as green vegetation, could be identified as strong red color in FCC image, and have association with the creeks. Spectrally, this feature could be identified by its high difference between red spectral absorption and NIR reflectance, due to the photosynthesis activity (Fig.

4). NPV, on the other hand, usually lacked significant quantities of chlorophyll and thus lacked the high NIR to red contrast.

Deep heavy gray and brown cracking clays were the typical soil color in this area [Accad *et al.*, 2006; Commonwealth of Australia, 2007]. Thus, the exposed soil class could be identified visually using true color image as it would showed the same color as in the field. In addition, the use of soil spectral reflectance was also critical in selecting this class. Features with a consistent 'soil like' reflectance profile throughout the image would be assigned as exposed soil class. However, the gray color in the image did not match up with the typical soil reflectance profile. On the other hand, the bright spots in the image had similar reflectance profile with soil. These spots could be exposed gray soil with highly reflectance during daytime.

Asphalt road has a relatively low and steady spectral signature throughout the wavelength (Fig.4). According to [Herold & Roberts, 2005], this low reflectance is due to the domination of hydrocarbon absorption in this material. However, asphalt pavement aging and erosion of the asphalt mix result in a gradual transition from hydrocarbon to mineral absorption characteristics with a general increase in brightness and changes in distinct small-scale absorption features.

Classification Result

Linear Spectral Unmixing determined the relative abundances of materials that were depicted in multi- or hyper-spectral imagery based on the materials' spectral characteristics. The reflectance at each pixel of the image was assumed to be a linear combination of the reflectance of each material (or end member) present within the pixel [Kruse *et al.*, 1993]. So given the resulting spectrum (the input data) and the end member spectra, the linear unmixing solved the abundance values of each end member for every pixel.

The results of spectral unmixing appeared as a series of gray-scale images, one for each end member (Fig.5), plus a root-mean-square (RMS) error image (Fig. 6b). Higher abundances (or higher errors for the RMS error image) were represented by brighter pixels. The unmixing results should have a data range (representing end member abundance) from 0 to 1. However, negative values and values greater than one were possible. The results were depending on the input end members, they changed if the end members were changed. The RMS error image helps to determine areas of missing or incorrect end members.

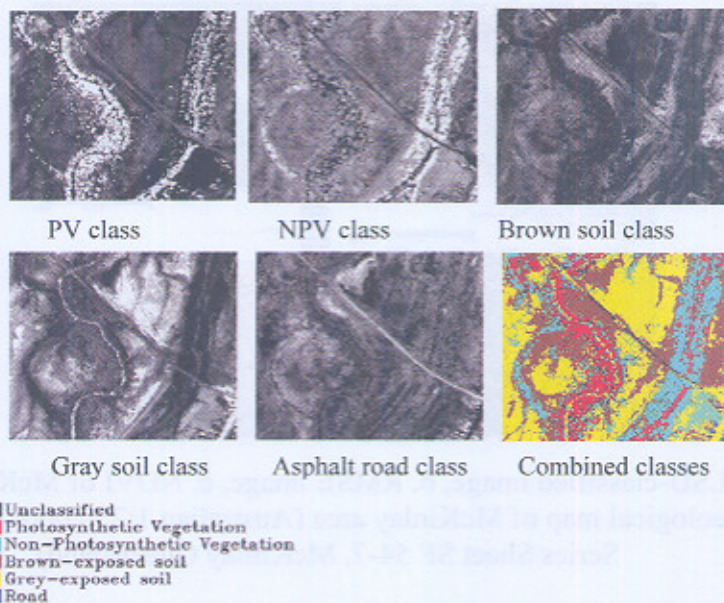


Figure 5. LSU images of each class and combined class

The result map show that PV and NPV classes were distributed along the river and creeks; brown-exposed soil dominated eastern part of image, while gray-exposed soil mostly found in west. The soil features' distribution was in parallel to the geological map of this area (Fig. 6d). From the statistics (Table 2), brown-exposed soil class dominated the area by covering 49.33% of the area, followed by gray-exposed soil at 30.80%. On the other hand, PV only occupied area of 5.75% and NPV of 12.58%. The soil features were dominant in this classification method. However, apart from the classification method applied, this was a typical arid and semi-arid environment, in which exposed soils were usually the largest contributor to the scene reflectance and dominate pixel responses [Lewis, 2000]. Vegetation features (PV and NPV), as earlier discussed, only covered small area in this environment. According to the properties of classes resulted (mainly shape, site, association, and distribution), LSU proven to be a powerful and efficient method of classification. However, the unclassified resulted from this classification was 1.43%. Those pixels were outside the threshold ranges defined for each class.

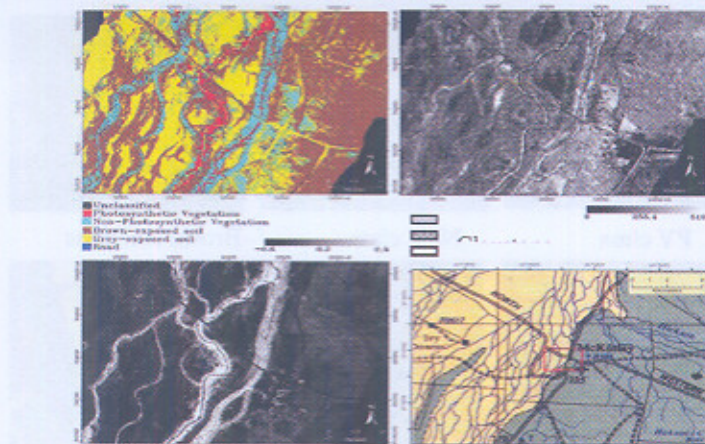


Figure 6. a. LSU-classified image, b. RMSE image, c. NDVI of McKinlay, and d. Geological map of McKinlay area (Australian 1:250,000 Geological Series Sheet SF 54-7, McKinlay Queensland)

Table 2. Statistics of LSU-classified image

Class	Pixel	Total	Pct	Acct Pct
Unclassified	3436	3436	1.43%	1.43%
PV	13844	17280	5.75%	7.18%
NPV	30292	47572	12.58%	19.76%
Brown soil	118738	166310	49.33%	69.09%
Gray soil	74139	240449	30.80%	99.89%
Road	276	240725	0.11%	100.00%

There were two factors possibly influencing the unclassified result. First, the non-linearity of mixed features, as reported by [Roberts *et al.*, 1993] that spectral mixture that includes green vegetation has the potential of being non-linear. It is due to transmission and scattering of NIR light by green leaves and the high spectral contrast between red and NIR of leaves. Second, this could be caused by inaccuracy of the threshold value assigned to the feature classes when creating a combination image. According on the RMSE image (Fig.6b), the largest contribution to these errors was found in areas insufficiently described by the unmixing model, such as river water bodies, some NPV classes, and some exposed soil spots.

Accuracy Assessment

Thematic information extracted from remote sensing images always contains error. This stage was conducted to ascertain whether each category in a classification really presents at the points specified on a map, and the boundaries separating categories valid as located [Jensen, 2005]. Several standard steps should be followed to assess the resulted image. However, because of the limitation in sample points, those procedures could not be conducted. Alternatively, a qualitative

matching was carried out between pictures of sample points and corresponding classification map results (Fig. 7). The classification accuracy resulted from LSU was then compared to the result of MLC as a standard per-pixel classification.

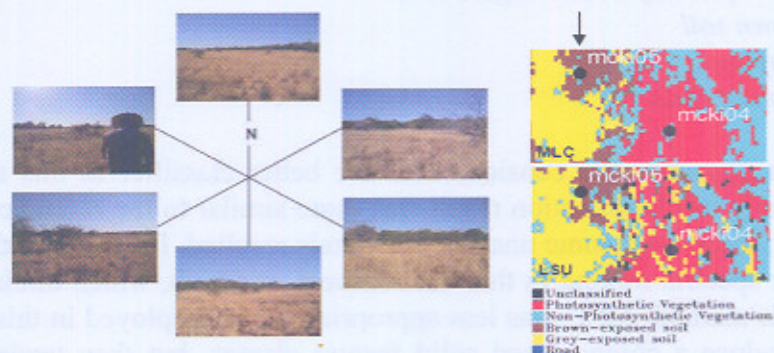


Figure 7. Sample pictures and classification results of point mcki 05

According to qualitative assessment, PV features were relatively well mapped in this classification approach, indicated by matched up features with the field photographs and data. NPV features were obstructed with the domination of exposed soil reflectance, but less than MLC did. Hence, the result experienced misclassification of these features. Up to this point, with the limitation of sample points, LSU has successfully mapped the PV and NPV.

Post-classification change detection was carried out to provide "matched classification" information between LSU and MLC as the standard classification. This is aimed to understand the degree of correspondence between those different classification approach (sub-pixel and per-pixel). In Table 3, the pixels that have matched classification on both images were located along the major diagonal of the matrix. The resulted percentage of matching classes was 70.6%, which meant they have a relatively high degree of correspondence. The unmatched class was more likely to occur in the middle and east part of the study area, particularly around the settlement area, where their end members were not assigned.

Table 3. Post-classification comparison matrices

		LSU						
		Uncl	PV	NPV	BS	GS	AR	Total
MIC	Uncl	3436						3436
	PV		9909	1231	211	462	130	11943
	NPV		3826	18036	10281	6832	36	39011
	BS		109	8768	102090	26535	17	137519
	GS		0	2256	5924	39893	93	48166
	AR		0	1	232	417	0	650
	Total Pixel							240725
	Matched Pixel			9909	18036	102090	39893	0
% Match								70.6

Legend:*Uncl* = unclassified,*PV* = photosynthetic vegetation*NPV* = non-photosynthetic vegetation,*BS* = brown soil*GS* = gray soil,*AR* = asphalt road

In general, LSU considered as the better classifier in this study, because semantically its classification result was more similar to the reference information. However, there were some unclassified pixels resulted. In addition, the potential of nonlinear spectral mixing in this environment was high, which diminished the utility of this method. MLC was less appropriate to be employed in this environment. It did produce a compact and solid feature classes, but they tended to be over-estimate, especially the soil features. It was obvious because all pixels in MLC were assigned according to the highest probability to the training area, which was a typical of hard classifier. Thus, many pixels would be forced into a certain class member, which was subject to misclassification.

CONCLUSION

Selection of the end member is the most important step for hyper-spectral classification since choosing a wrong one can make great difference in classification result. The use of ancillary information is proven to be very useful as guidance in selecting appropriate end member. The classification result indicated that PV and NPV features were well identified in LSU. Exposed soils were dominating the spectral reflectance of this area, especially when mixing with NPV features. According to post-classification comparison with MLC, there was a relatively high correspondence result between them (70.6%). However, a quantitative accuracy assessment showed that LSU classified image has greater match with the field data. Up this point, this classification technique is proven to be successful in discriminating PV, NPV, and exposed soils in the semi-arid area. Nevertheless, LSU experienced with some unclassified pixels. It should be note that this technique depends on the threshold value of rule images determined by user. Some possible sources of error might affect classification results, such as impurity of end members and the nonlinearity of features' reflectance.

ACKNOWLEDGEMENT

The HyMap dataset for this study were supported by The Centre of Remote Sensing and Spatial Information Science, The University of Queensland Australia, as well as the field data. The author wishes to thank Professor Stuart Phinn for the image analysis discussions.

REFERENCES

- Accad, A., Neldner, V. J., Wilson, B. A. & Niehus, R. E (2006), *Remnant Vegetation In Queensland, analysis of remnant vegetation 1997-1999-2000-2001-2003, including regional ecosystem information [CD-ROM]*, Queensland Herbarium, Environmental Protection Agency, Brisbane.
- Asner, G. P. & Heidebrecht, K. B (2002), Spectral unmixing of vegetation, soil and dry carbon cover in arid regions: comparing multispectral and hyper spectral observations, *International Journal of Remote Sensing*, 23(19), 3939-3958.
- Bastin, G. N. & Ludwig, J. A (2006), Problems and prospects for mapping vegetation condition in Australia's arid rangelands, *Ecological Management & Restoration*, 7(S1), S71-S74.
- Commonwealth of Australia (2007), *Australian Natural Resources Atlas V2.0* [Online] Available at www.environment.gov.au/atlas.
- Cocks, T., Jansen, R., Stewart, A, Wilson, I. & Shields, T. (1998), *The HyMap Airborne Hyper spectral Sensor: The System, Calibration and Performance*, Article presented at 1st EARSEL Workshop on Imaging Spectroscopy, Zurich.
- Drake, N. A., Mackin, S. & Settle, J. J (1999), *Mapping vegetation, soils, and geology in semi-arid scrublands using spectral matching and mixture modeling of SWIR AVIRIS imagery*, *Remote Sensing of Environment*, 68(1), 12-25.
- Herold, M. & Roberts, D. A (2005), *Mapping Asphalt Road Conditions with Hyper spectral Remote Sensing*, [Online] available at http://www.isprs.org/commission8/workshop_urban/herold_roberts.pdf.
- Hill, M. J., Asner, G. P. & Held, A. A (2006), *the bio-geophysical approach to remote sensing of vegetation in coupled human-environment systems – societal benefits and global context*, *Journal of Spatial Science*, 52(2), 49-66.
- Jensen, J. R (2005), *Introductory Digital Image Processing: a remote sensing perspective*, 3rd end, Pearson Prentice Hall, Sydney.
- Karnieli, A., Gabai, A., Ichoku, C., Zaady, E. & Shachak, M. (2002), *Temporal dynamics of soil and vegetation spectral responses in a semi-arid environment*, *International Journal of Remote Sensing*, 23(19), 4073-4087.
- Kruse, F. A., Lefkoff, A. B., Boardman, J. W., Heidebrecht, K. B., Shapiro, A. T., Barloon, P. J. & Goetz, A. F. H (1993), *The Spectral Image Processing System (SIPS) – Interactive Visualization and Analysis of Imaging Spectrometer Data*, *Remote Sensing of Environment*, 44(2-3), 145-163.

- Kruse, F. A., Boardman, J. W., Lefkoff, A. B., Young, J. M. & Kierein-Young, K. S (2000). *HyMap: an Australian Hyper spectral Sensor Solving Global Problems – Results from USA HyMap Data Acquisition*, [Online] available at www.hgimaging.com/PDF/kruse_10ARSPC_hymap.pdf.
- Lewis, M (2000), *Discrimination of arid vegetation composition with high resolution CASI imagery*, *Rangeland Journal*, 22(1), 141-167.
- Lewis, M., Jooste, V. & de Gasparis, A. A (2001), *Discrimination of arid vegetation with airborne multispectral scanner hyper spectral imagery*, *IEEE Transaction on Geosciences and Remote Sensing*, 39(7), 1471-1479.
- Lillesand, T. M., Kiefer, R. W. & Chipman, J. W (2004), *Remote Sensing and Image Interpretation*, 5th edn, John Willey & Sons, New York.
- McGwire, K., Minor, T. & Fenstermaker, L (2000), *Hyper spectral mixture modeling for quantifying sparse vegetation cover in arid environments*, *Remote Sensing of Environment*, 72(3), 360-374.
- Okin, G. S., Roberts, D. A., Murray, B. & Okin, W. J (2001), *Practical limits on hyper spectral vegetation discrimination in arid and semi-arid environments*, *Remote Sensing of Environment*, 77(2), 212-225.
- Research System Inc (2003), *ENVI Online Manuals and Tutorials*, RSInc. Colorado.
- Roberts, D. A., Smith, M. O. & Adams, J. B (1993), *Green vegetation, No photosynthetic Vegetation, and Soils in AVIRIS Data*, *Remote Sensing of Environment*, 44(2-3), 255-269.
- Rosso, P. H., Ustin, S. L. & Hastings, A (2005), *maps marshland vegetation of San Francisco Bay, California, using hyper spectral data*, *International Journal of Remote Sensing*, 26(23), 5169-5191.
- Tueller, P. T (1987), *Remote sensing science applications in arid environments*, *Remote Sensing of Environment*, 23(2), 143-154.
- Ustin, S. L., Roberts, D. A., Gamor, J. A., Asner, G. P. & Green, R. O (2004), *Using imaging spectroscopy to study ecosystem processes and properties*, *Bioscience*, 54(6), 523-534.
- Van der Meer, F. D. & de Jong, S (Ed) (2001), *Imaging Spectrometry, basic principles and prospective applications*, Kluwer Academic Publishers, Dordrecht.
- Yang, C., Everitt, J. H. & Bradford, J. M (2006), *Use of Spectral Angle Mapper (SAM) and hyper spectral Imagery for Yield Estimation an ASABE Meeting Presentation*, paper number: 061168, Miami.